# Obstacle avoidance in highly automated cars: can progressive haptic shared control make it safer and smoother?

Béatrice Pano, Philippe Chevrel, Fabien Claveau, Chouki Sentouh, Franck Mars

# Obstacle avoidance in highly automated cars: can progressive haptic shared control make it safer and smoother?

Béatrice Pano, Philippe Chevrel, Fabien Claveau, Chouki Sentouh, Franck Mars

**Haptic shared control has proven to be an effective method to assist a driver in controlling a vehicle. This method is now being considered for use in developing strategies for smooth transitions between manual and autonomous driving modes. This paper has two objectives. First, it proposes to adapt an existing haptic shared control strategy to achieve transitions between manual and autonomous modes and to evaluate this approach with real drivers on a driving simulator. Second, it proposes to evaluate four different transition profiles in an obstacle avoidance context. The first profile is a gradual transition from autonomous mode to shared control mode, followed by another transition from shared control mode to autonomous mode once the obstacle is passed. The second is a gradual transition from autonomous mode to manual mode. The third is a binary transition from autonomous mode to manual mode. Finally, in the fourth condition, the driver overrides the autonomous mode. These transition profiles were evaluated in curves and straight lines on a driving simulator. The results first validated the use of the haptic shared control strategy to execute transitions between manual and autonomous modes. The distribution of the torques delivered by the automation system and the driver corresponded to the progression of the expected sharing level. Second, the gradual transitions showed advantages over binary transitions and the override of the autonomous mode, both in terms of steering performance and subjective evaluation.**

***Index Terms*—Haptic control, Human-automation interaction, Autonomous vehicles.**

## I. Introduction

In recent years, the development of autonomous vehicles has become a major interest for car manufacturers. As human error remains the primary factor in the number of car accidents [1], the autonomous vehicle can be considered as a means of improving road safety [2]. However, in the early stages of autonomous vehicle deployment, the driver will still need to be able to regain control because vehicles will not be able to handle certain complex or unexpected situations. Therefore, the question of transitions between autonomous and manual driving is a central issue in the development of the next generation of vehicles.

The transition from autonomous driving to manual driving is a critical phase. The driver needs to be aware of the driving situation in order to regain control properly, as the driver's workload suddenly increases during the transition [3]. However, the higher the previous level of automation, the less attentive the driver may have been to the road before the takeover request, especially if they were involved in secondary tasks [4] [5] [6] [7]. The reason for this inattention is that drivers may become complacent with the autonomous system, which works well most of the time. The reduction of the driver's attention to the road may lead to a decrease in the ability to regain manual control [8] [9]. Therefore, in order to achieve good recovery performance, drivers need sufficient time to regain situational awareness. In addition, after a phase of autonomous driving, the driver needs to restore eye-steering coordination and recalibrate the sensorimotor loops involved in the control of the actuators [10]. Therefore, research is being conducted to determine which modalities are most relevant for smooth transitions [11] [12] [13].

Haptic shared control (HSC) could be a satisfactory solution to manage transitions [14] [10]. In HSC, to avoid abrupt transitions and to switch gradually from one driving mode to the other, autonomous driving and manual driving can be connected through a phase in which the driver and the automation system share the steering wheel [15]. When used as a driving assistance system, HSC has been shown to reduce driver workload and increase vehicle stability [16]. Several HSC strategies have been proposed in the literature to achieve transitions [17] [18] [19]. In [19], a comparison of different transition profiles using HSC was evaluated in a context of takeover request initiated by the machine in the lane-following task. The study shows the benefit of using a gradual transition in such a case as results are better in terms of lane following performance as well as driver acceptance.

The objective of this study is two-fold. First, it proposes to adapt the HSC strategy presented in [20] to the problem of transitions and to implement it in a driving simulator for evaluation with real drivers. Second, an experiment was conducted to compare different transition profiles in order to determine their potential usefulness. Four transition profiles were assessed in the context of obstacle avoidance, in both curves and straight lines. Two of these transition profiles involve transitions from autonomous mode to manual mode: a gradual linear transition and a binary transition. The other two profiles end in autonomous mode. The first of the other two profiles is a gradual transition from autonomous driving mode to HSC of the steering wheel that lasts a few seconds before returning to autonomous mode. The second remains in autonomous mode for the duration of obstacle avoidance with the possibility for the driver to override the system.

The rest of this article is organised as follows. Section II presents the HSC strategy used and how it has been adapted to

Béatrice Pano, Philippe Chevrel and Fabien Claveau are with Laboratoire des Sciences du Numérique de Nantes (LS2N UMR CNRS 6004), IMT-Atlantique, 44307 Nantes, France, e-mails : firstname.lastname@ls2n.fr

Chouki Sentouh is with Laboratoire d'Automatique, de Mecanique et d'Informatique industrielles et Humaines (LAMIH UMR CNRS 8201), Université Polytechnique Hauts-de-France, 59300 Valenciennes, France, e-mail: Chouki.Sentouh@uphf.fr

Franck Mars is with Laboratoire des Sciences du Numérique de Nantes (LS2N UMR CNRS 6004), CNRS & Centrale Nantes, 44321 Nantes, France, e-mail: Franck.Mars@ls2n.fr

achieve progressive transitions. Section III presents the whole experimental procedure. It contains a description of the equipment used, the participants, the experimental procedure, and the indicators that will be used to analyse the results. Finally, the results are described in Section IV before concluding in Section V.

## II. Transition between manual and autonomous driving using haptic shared control

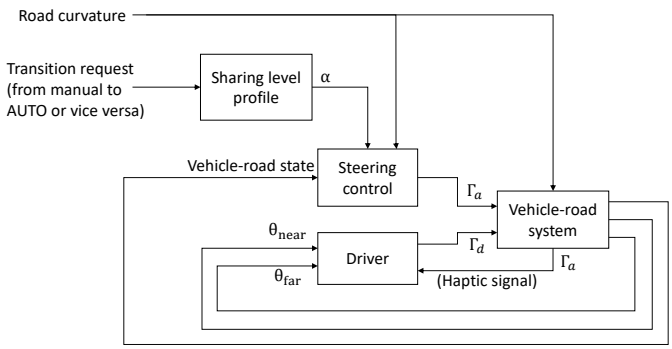


Fig. 1. Shared control based transition principle

In order to achieve progressive transitions between manual and autonomous driving, the use of an HSC strategy is proposed. Figure 1 illustrates the principle of the solution investigated in this paper. The steering control system (respectively the driver) is driving alone in autonomous (respectively manual) driving. In case of a request (from the driver or from the system according to the environment), the level of sharing gradually changes to autonomous or manual driving. This section first introduces the driver-vehicle-road model used for control synthesis and associated signals, and then the control strategy.

### A. Description of models

The control strategy designed in the current work is based on two models: a vehicle-road model and a driver model. The vehicle-road model represents both the vehicle dynamics and its position on the road using for a given longitudinal speed. It can be written as follows:

$$\dot{x}_{vr} = A_{vr}x_{vr} + B_{1vr}(\Gamma_a + \Gamma_d) + B_{2vr}\begin{bmatrix} F_w \\ \rho_{ref} \end{bmatrix} \quad (1)$$

with:

$$A_{vr} = \begin{bmatrix} a_{11} & a_{12} & 0 & 0 & \frac{b_1}{R_s} & 0 \\ a_{21} & a_{22} & 0 & 0 & \frac{b_2}{R_s} & 0 \\ 0 & 1 & 0 & 0 & 0 & 0 \\ v_x & l_s & v_x & 0 & 0 & 0 \\ 0 & 0 & 0 & 0 & 0 & 1 \\ \frac{T_{s\beta}}{I_s} & \frac{T_{sr}}{I_s} & 0 & 0 & -\frac{T_{s\beta}}{R_s I_s} - \frac{\mu_s}{I_s} & -\frac{B_s}{I_s} \end{bmatrix} \quad (2)$$

TABLE I
Vehicle-Road model parameters values

| | | |
|---|---|---|
| $l_f$ | Distance from gravity center to front axle | 1.289m |
| $l_r$ | Distance from gravity center to rear axle | 1.611m |
| $m$ | Total mass of the vehicle | 1834.9kg |
| $J$ | Vehicle yaw moment of inertia | 2800kg.m$^2$ |
| $C_{f0}$ | Front cornering stiffness | 64807N/rad |
| $C_{r0}$ | Rear cornering stiffness | 68263 N/rad |
| $\eta_t$ | Tire length contact | 0.245m |
| $\nu$ | Adhesion | 0.8 |
| $K_m$ | Manual steering column gain | 0.031 |
| $R_s$ | Steering-gear ratio | 14.54 |
| $B_s$ | Steering-system damping coefficient | 1.0173 |
| $I_s$ | Inertial moment of steering system | 0.0891kg.m$^2$ |
| $\mu_s$ | Spring stiffness | 0.9141N.m/rad |
| $l_s$ | Look-ahead distance | 5m |
| $V_x$ | Longitudinal speed | 18m.s$^{-1}$ |
| $D_{far}$ | Distance to the tangent point | 15m |

$$B1_{vr} = \begin{bmatrix} 0 \\ 0 \\ 0 \\ 0 \\ 0 \\ \frac{1}{I_s} \end{bmatrix}, B2_{vr} = \begin{bmatrix} e_{11} & 0 \\ e_{22} & 0 \\ 0 & -v_x \\ 0 & -l_s v_x \\ 0 & 0 \\ 0 & 0 \end{bmatrix} \quad (3)$$

where $\Gamma_a$ and $\Gamma_d$ respectively, are the assistance and the driver torque applied on the steering wheel; $\rho_{ref}$ the road curvature; and $F_w$ the wind force resultant applied on the vehicle. The vehicle-road state vector is defined as $x_{vr} = \begin{bmatrix} \beta & r & \psi_L & y_L & \delta_d & \dot{\delta}_d \end{bmatrix}$, where $\beta$ is the slip angle, $r$ is the yaw rate, $\psi_L$ is the heading error angle, $y_L$ is the lateral deviation between the vehicle and the lane centre at a look-ahead distance $l_s$, and $\delta_d$ is the steering wheel angle. Coefficients $a_{11}$, $a_{12}$, $a_{21}$, $a_{22}$, $b_1$, $b_2$, $T_{s\beta}$, $T_{sr}$, $e_{11}$, and $e_{22}$ are described in [21]. Vehicle-road model parameter values are given in Table I.

The use of a driver model is recommended to design an HSC acting in synergy with the driver. This reduces conflicts between the assistance system and the driver and improves driver acceptance [22] [23]. The driver model used in this document is the one proposed by [23]. This cybernetic driver model has two inputs: the angle to a near point, $\theta_{near}$, and the angle to a far point, $\theta_{far}$. These two points represent the use of visual information by drivers to compensate for lateral positioning errors and to anticipate changes in road curvature, respectively [24]. The driver model can be described as follows:

$$\begin{gathered} \dot{x}_d = A_d x_d + B_d \begin{bmatrix} \theta_{far} & \theta_{near} & \delta_d & \Gamma_s - \Gamma_a \end{bmatrix}^T \\ \Gamma_d = C_d x_d \end{gathered} \quad (4)$$

where $\Gamma_s$ is the self-aligning torque. The driver state vector, $x_d$, and matrices $A_d$, $B_d$, and $C_d$ can be found in [25] or [26].

### B. Haptic shared control strategy

In HSC, both the driver and the assistance can apply a torque to the steering column. The driver apply a torque $\Gamma_d$ through the steering wheel and the assistance apply a torque $\Gamma_a$ through a motor on the steering column. The HSC synthesis aims at finding the assistance torque to be applied

TABLE II
DRIVER MODEL PARAMETERS

| | | |
|---|---|---|
| $K_p$ | Anticipation gain | 3.4 |
| $K_c$ | Compensation gain | 15 |
| $T_I$ | Compensation frequency band | 1 |
| $T_L$ | Compensation rate | 3 |
| $\tau_p$ | Human processing time delay | 0.04 |
| $K_r$ | Steering column stiffness | 1 |
| $K_t$ | Steering-wheel holding stiffness | 12 |
| $T_N$ | Neuromuscular time constant | 0.1 |

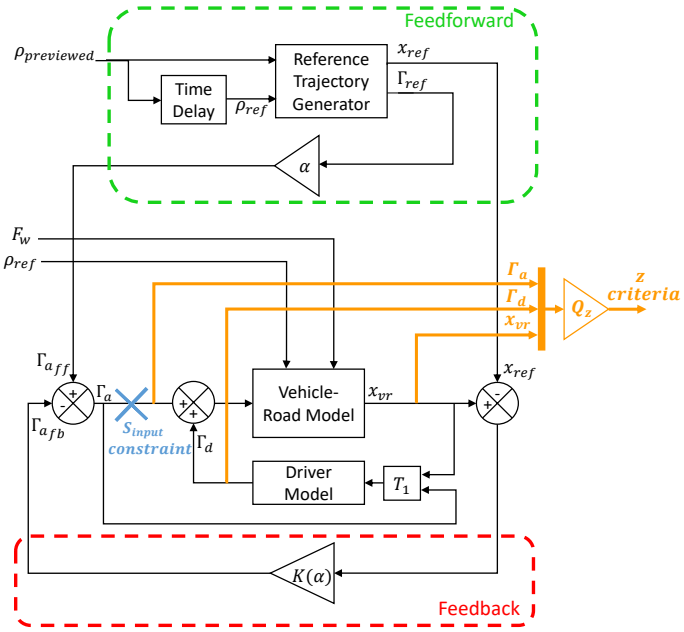


Fig. 2. Haptic shared control strategy

in order to fulfill some objectives. Here, the assistance torque must be calculated to conform to a certain sharing level, $\alpha$, which is the expected percentage of steering torque provided by the assistance system relative to the total torque applied to the steering wheel. Moreover, the assistance should allow for accurate lane following and respect the driver's comfort. The proposed HSC strategy is divided into two sequentially designed parts: a "feedforward" part with an anticipatory action and a "feedback" part with a compensatory action. This control strategy is illustrated in Figure 2. Block T1 represents the calculation of the inputs to the driver model $\begin{bmatrix}\theta_{far} & \theta_{near} & \delta_d & \Gamma_s - \Gamma_a\end{bmatrix}^T$. The feedforward part, which is shown in the green dotted rectangle in Figure 2, is composed of a trajectory generator. The latter has one input, the curvature of the road ahead of the vehicle (previewed at a time t, $\rho_{previewed}(t) = \rho_{ref}(t + T_{horizon})$ with $T_{horizon} = 2s$), and the reference trajectory ($\Gamma_{ref}$ control input, and state $x_{ref}$) as output vector. These outputs are calculated by simulating an autonomous virtual vehicle based on the vehicle-road model (1), following the same road as the real vehicle. This virtual vehicle is driven by a $H_2$-preview strategy that was developed in [27], a controller that provides accurate lane following performance but does not take into account driver preferences. The feedback part is shown in the red dotted rectangle in Figure 2 and consists of a $H_2/H_\infty$ regulator applied to the difference between the real road vehicle state, $x_{vr}$, and the virtual state, $x_{ref}$ :

$$\begin{aligned}\Gamma a_{fb} &= K.Y_{diff} \\ &= k_\beta \beta_{diff} + k_r r_{diff} + k_{\psi_L}\psi_{L_{diff}} + k_{y_L} y_{L_{diff}} \\ &+ k_{\delta_d}\delta_{d_{diff}} + k_{\dot{\delta}_d}\dot{\delta}_{d_{diff}}\end{aligned} \quad (5)$$

with $Y_{diff} = x_{vr} - x_{ref} = \begin{bmatrix}\beta_{diff} & r_{diff} & \psi_{L_{diff}} & y_{L_{diff}} & \delta_{d_{diff}} & \dot{\delta}_{d_{diff}}\end{bmatrix}$.

Feedback gains $K = \begin{bmatrix}k_\beta & k_r & k_{\psi_L} & k_{y_L} & k_{\delta_d} & k_{\dot{\delta}_d}\end{bmatrix}$ are calculated by solving the optimisation problem $(P)$.

$$P : \begin{cases} \text{Find K such as:} \\ \quad min_K(||T_{(\rho_{previewed},F_w)\to z}||_2) \\ \text{under constraints:} \\ \quad ||S_{input}||_\infty \leq S_{max} \end{cases} \quad (6)$$

With $S_{input}$ the system input sensitivity and $z$ the performance vector:

$$z = Q_z \begin{bmatrix}\psi_L & y_{CG} & a_{lat} & (1-\alpha)\Gamma_a - \alpha\Gamma_d & \Gamma_d & \Gamma_a\end{bmatrix}^T \quad (7)$$

Where $Q_z$ is a weighting matrix and $y_{CG}$ is the lateral deviation at the vehicle center of gravity. The performance vector $z$ is chosen to ensure precise lane following performance, driver comfort and good sharing performance.

Steering control sharing relies on the controller parameterization at two different places, indicated in Figure 2. For the feedforward part it allows to select part of the reference torque ($\Gamma_{aff} = \alpha\Gamma_{ref}$). For the feedback part, the sharing level is included during the synthesis process through the chosen criteria (see eq. 7). As a result, it parameterizes all the feedback gains. This HSC strategy was tested on Simulink in Matlab using a driver model to drive the vehicle [20]. The simulation was performed with a fixed sharing level, $\alpha$, and the results showed accurate lane-following and few conflicts between the assistance system and the driver model.

### C. Progressive transition using haptic shared control

In order to use the HSC introduced in Section II-B to make the transition between manual and autonomous driving, we need to be able to change the sharing level, $\alpha$, while driving.

To resolve this point, feedback gains $K = \begin{bmatrix}k_\beta & k_r & k_{\psi_L} & k_{y_L} & k_{\delta_d} & k_{\dot{\delta}_d}\end{bmatrix}$ (see (5)) were synthesised for different sharing levels ($\alpha = \begin{bmatrix}0.1 & 0.2 & 0.3 & 0.4 & 0.5 & 0.6 & 0.7 & 0.8 & 0.9\end{bmatrix}$). Feedback gains chosen for manual mode ($\alpha = 0$) were $K = \begin{bmatrix}0 & 0 & 0 & 0 & 0 & 0\end{bmatrix}$ as there is no assistance in this mode. For autonomous mode ($\alpha = 1$), the $K$ vector was calculated using LQI (linear quadratic with integral action) synthesis. The integral action relates to $y_L$ and makes lane-following more accurate. Starting from the set of gain vectors thus calculated, we did a polynomial interpolation with $10^{th}$-order polynomials. Notice that other interpolation approaches could accomplish the same tasks as the gains had a quasi-linear relationship between points. The resulting interpolation smoothly links the shared control solutions from

purely manual to fully automated driving, and shows the absence of any over-parameterization.

The level of sharing is a function of the selected transition profile and the location of the vehicle since the transitions were initialised at specific positions in the scenarios (see procedure).

## III. Experiment

### A. Participants

Seventeen participants took part in the experiment (6 women and 11 men), aged 24 to 53 years (mean = 30.94, SD = 8.20). They had at least 3 years of driving experience and travelled an average of 12,550 km per year (SD = 10,644 km). Each participant signed a consent form prior to the experiment. The study was reviewed and approved by the non-interventional research ethics committee of Nantes University (CERNI, IRB #IORG0011023, decision #08072021-2).

### B. Equipment

Fig. 3. Driving simulator (SCANeR-AVSimulation)

This experiment was carried out using a fixed-base driving simulator (SCANeR Studio, AVSimulation) composed of a dashboard, a gear lever, three pedals (accelerator, brake and clutch), an adjustable seat, a steering wheel, and a TRW steering system. The driver could see the visual environment on three LCD screens that cover a visual angle of 115 °horizontally and 25 °vertically. The vehicle model used corresponds to a Citroën C5. A motor was used to apply the assist torque to the steering column, which was equipped with a torque sensor. Specifically, the sensor measured the torsion of the column on a specific section between the steering wheel and the motor responsible for providing the torque feedback and the assistance torque. This information allowed to estimate the driver torque applied to the steering wheel, with a small inaccuracy due to residual friction. A human-machine interface (HMI) was used to communicate with the driver, consisting of a touch screen placed on the right side of the steering wheel.

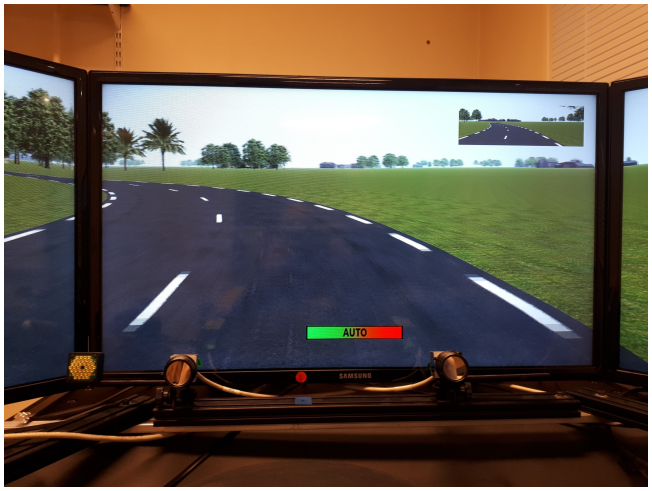


Fig. 4. Centre screen of the simulator displaying the progressive bar while in autonomous mode

### C. Procedure

Throughout the experiment, three different control modes were used: manual mode, shared control mode, and autonomous mode. In manual mode, the only torque applied to the steering wheel is that of the driver. In shared control mode, the torque applied to the steering wheel is the assistance torque added to the driver's torque. The contribution of the assistance torque depends on the sharing level. In autonomous mode, the driver had to release the steering wheel, and the only torque applied was the assistance torque. These modes only concerned the steering task, not the longitudinal control of the vehicle, as the vehicle speed was set using cruise control.

The steering mode was communicated to the participants in two ways. First, the HMI on the right side of the steering wheel informed the participants about the driving mode. Second, a progress bar, that is shown in Figure 4, was displayed at the bottom of the central screen superimposed on the visual scene. This progress bar represented the sharing level. In autonomous mode, the bar was fully coloured and the word "AUTO" appeared in its centre. The participants were instructed to release the steering wheel and let the assistance drive autonomously only under this condition. The experiment was conducted in three steps, described below.

#### 1) Preliminary phase

The experiment began with a familiarisation period. Participants were explained how to drive the simulator. The participants were instructed to accelerate until the vehicle reached the speed limit of 18 m/s. From that moment, they had to release the accelerator and the clutch pedal while continuing to control the steering wheel until the end of the simulation: that is, for about 10 minutes.

#### 2) First experimental phase

During the first phase of the experiment, the participants drove on a track composed of successive turns of 75 m or 95 m radius of curvature (see Figure 5). Before the simulation, the principle of shared control and the transition procedure were explained to the participants. Initially, the participants drove in manual mode. After a few metres, a sound and an indication on

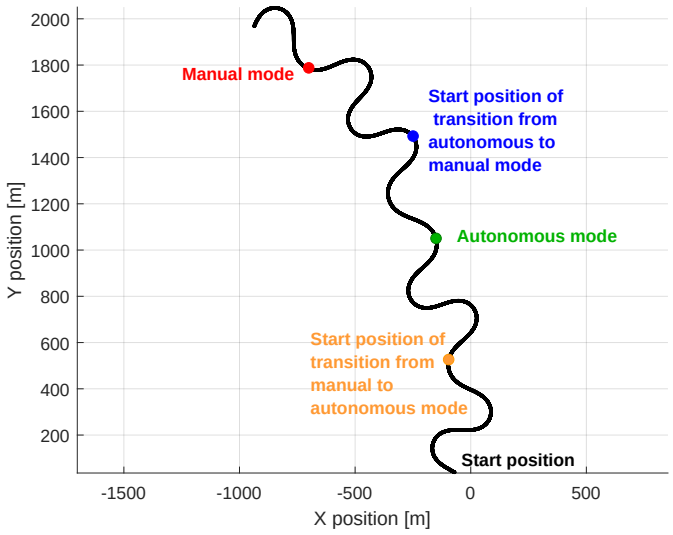


Fig. 5. Track for the first experimental phase

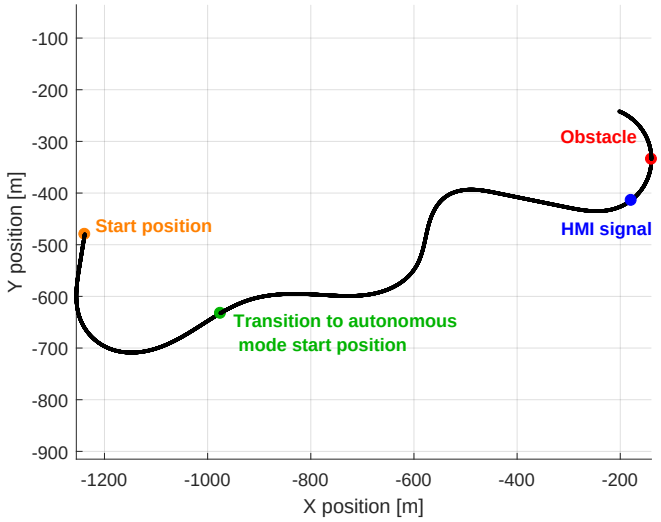


Fig. 6. Curve scenario track

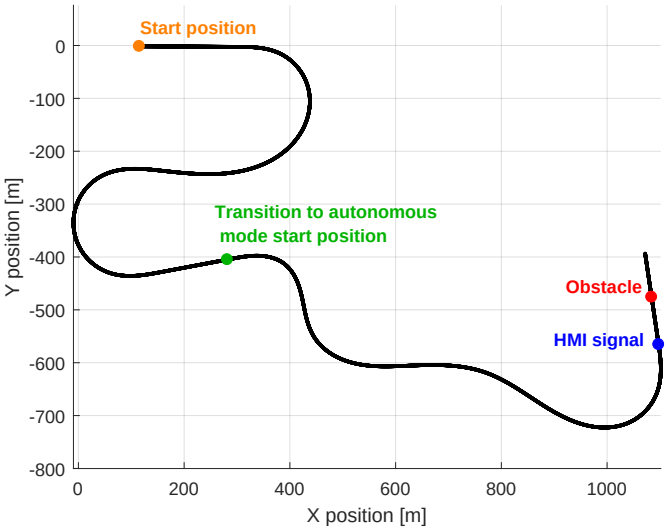


Fig. 7. Straight-line scenario track

Fig. 8. Obstacle

the HMI warned the participants that a transition from manual to autonomous mode was about to start. The transition lasted 50 seconds, and participants were informed of the evolution of the sharing level by a progress bar. When the autonomous mode was reached, participants had to release the steering wheel. After 590 metres in autonomous mode, a new signal warned that a second transition was beginning, this time from autonomous to manual mode, again within 50 seconds. The purpose of this experimental phase was to allow participants to become familiar with control transitions and allow them a considerable period of time to feel the progressiveness of the system. The phase also allowed validation of the control law by checking that the actual repartition between the driver and the system corresponded to the desired repartition. To assess this distribution, an estimate of the instantaneous sharing level was used, which is calculated as follows:

$$\alpha_{calculated} = \frac{|\Gamma_a|}{|\Gamma_a| + |\Gamma_d|} \tag{8}$$

*3) Second experimental phase*

The second phase of the experiment consisted of a test of four transition profiles in an obstacle-avoidance situation. The obstacle avoidance situation occurred while the vehicle was in autonomous mode and the driver was involved in a secondary task. Then, as the assistance was not designed to avoid the obstacle, the driver had to regain control of the vehicle. Two scenarios were used with an obstacle placed either in a bend or a straight line. These scenarios will be refered to as the curve and straight-line scenarios respectively. They are depicted in Figure 6 and 7.

Each scenario consisted of three parts. Participants first drove in manual mode for around 560 metres for the curve scenario and 1,390 metres for the straight-line scenario. Then, a gradual transition to autonomous driving mode was initiated. Once the autonomous mode was reached, participants were asked to release the steering wheel and read aloud a text displayed on the HMI. To ensure that participants were no longer monitoring the driving situation, they were instructed

to avoid looking at the road while reading and to stop reading only if the HMI informed them that they should take control. After about 780 metres of reading for the curve scenario and 920 metres for the straight-line scenario, a takeover request was delivered. One second after the signal, one of the four transition profiles was activated, coinciding with the start of the obstacle-avoidance manoeuver.

The evolution of the sharing level, $\alpha$, during each of the tested transition profiles is illustrated on Figure 9. These four transition profiles can be described as follows:

- Transition 1: A progressive transition in 4 s from autonomous mode to shared control mode ($\alpha$ = 0.5); then, once the obstacle was passed, another transition of 4 s from shared control mode to autonomous mode.
- Transition 2: A progressive transition of 8 s from autonomous to manual mode
- Transition 3: A binary transition from autonomous to manual mode
- Transition 4: The vehicle remains in autonomous mode, but the assistance torque was limited to 5 N.m. The driver keeps the ability to override the system's action.

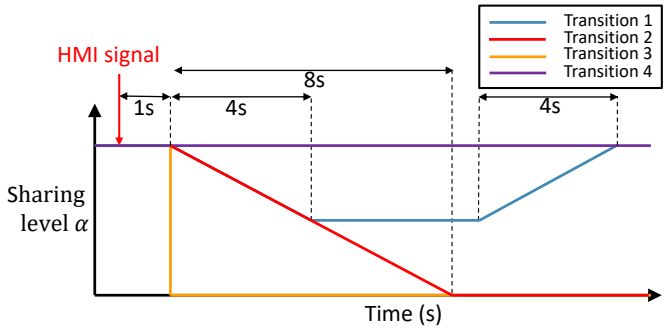


Fig. 9. Evolution of the sharing level for each transition profile

Each participant experienced the four transition profiles in a randomised order and each transition profile was verbally explained to the participants before the trials. For each transition profile, the participant had to drive three times, once with the transition in a bend (Figure 6), a second time in a straight line (Figure 7), and finally in a bend again (same condition as the first drive). The objective of repeating the curve scenario was to assess whether performance during transitions changed depending on whether the driver was surprised by (1st try) or habituated (3rd try) to the takeover.

After each condition, the participants had to answer four questions on Likert scales:

- Question 1: Did you feel that the transition was smooth (gradual and seamless)?
- Question 2: Did you feel that the assistance system helped you?
- Question 3: What was the level of intrusiveness of the system?
- Question 4: Did you get the impression that the system guaranteed your safety?

### D. Dependent variables

Objective indicators were used to assess the transition profiles.

- The steering wheel reversal rate, $SWRR$, which provides information on the stability of the steering control
- The maximum absolute lateral deviation, $max(|y_L|)$
- The mean absolute driver torque, $mean(|\Gamma_d|)$
- The metric $W$ in equations 9 to 12 represents the physical workload related to the driver's steering activities. From the viewpoint of energy consumption, this metric can be interpreted as the steering energy provided by the driver within a duration $T$ to perform a desirable steering maneuver [28] [29]. If the value of $W$ is positive, it is motor work and if negative, then it is resistant work. The positive and negative steering workload, $W_+$ and $W_-$ are respectively defined as:

$$W_+ = \int w_+(t)\,\mathrm{d}t \tag{9}$$

$$W_- = \int w_-(t)\,\mathrm{d}t \tag{10}$$

with:

$$w_+(t) = \begin{cases} \Gamma_d(t)\dot{\delta}_d(t) & \text{if } \Gamma_d(t)\dot{\delta}_d(t) \geq 0 \\ 0 & \text{else} \end{cases} \tag{11}$$

$$w_-(t) = \begin{cases} -\Gamma_d(t)\dot{\delta}_d(t) & \text{if } \Gamma_d(t)\dot{\delta}_d(t) < 0 \\ 0 & \text{else} \end{cases} \tag{12}$$

We used this objective index to evaluate the driver's comfort from the viewpoint of the driver's interaction with the assistance controller via the steering wheel. Such objective analysis using steering workload has been widely used directly or indirectly for driver comfort analysis in many steering assistance or shared control works [30] [31].

In addition, the scores measured on the four Lickert scales at the end of the experiment (see Section III-C3) provided 4 subjective indicators.

A repeated-measures ANOVA was carried out on each of these indicators in order to decide whether the transition profile had a significant effect. Tukey HSD tests were performed for posthoc comparisons. The results for the straight-line scenario were tested using one-way ANOVA with profile as the only independent variable. For curve scenarios, two-way ANOVAs were used with trial repetition as a second variable.

## IV. Results

### A. Preliminary validation of the shared control strategy

The analysis of the first phase of the experiment allows validation of the control strategy chosen for the transition between manual and autonomous driving. Figure 10 shows that as the required sharing level, $\alpha$, increases, the assistance torque also increases, as expected. This allows the participants to gradually release the steering wheel, resulting in a progressive decrease in driving torque. In addition, the lateral deviation curve shows that lane tracking was very accurate when the vehicle was in autonomous mode since the lateral deviation

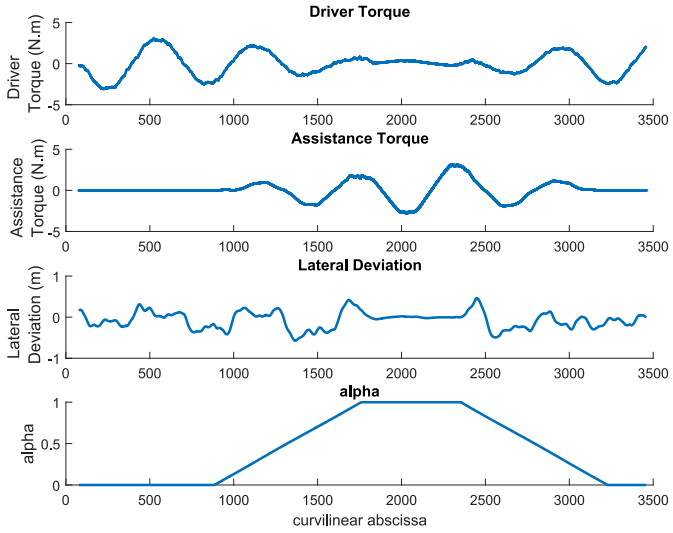


Fig. 10. Driver torque, assistance torque, and lateral deviation averaged across participants as a function of the curvilinear abscissa of the road during the first phase of the experiment. The evolution of the sharing level is shown in the bottom graph.

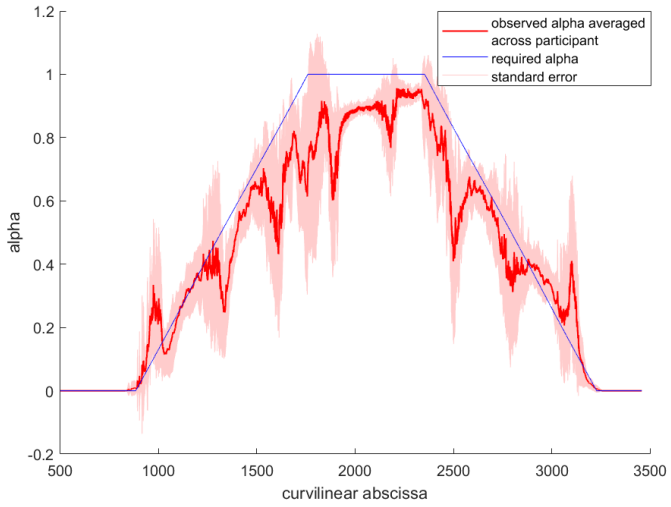


Fig. 11. Actual sharing level during the simulation averaged across participants compared with required sharing level

was close to 0. Figure 11 allows comparison of the required sharing level and the actual sharing level, varying over time, during the simulation. Note that the actual sharing level follows, on average, the requested level. The reason why the actual sharing level is not equal to 1 when in autonomous mode is that there is always a residual torque due to friction in the steering system that is measured by the sensor even if the driver releases the steering wheel.

In conclusion, this first test shows that the progressive transition strategy gives the expected results. Participants decreased their contribution to steering torque when $\alpha$ increased and gradually regained steering control when $\alpha$ decreased.

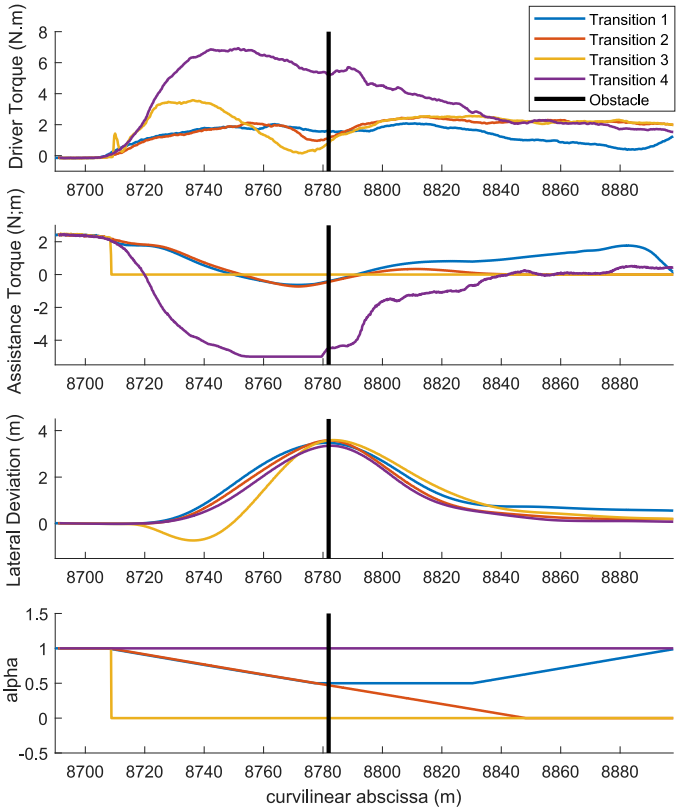


Fig. 12. Driver torque, assistance torque, and lateral deviation averaged across participants as a function of the road curvilinear abscissa in the curve scenario. The sharing level is shown in the bottom graph.

### *B. Transition profiles comparison*

#### *1) Objective indicators*

The second phase of the experiment aimed to compare the four transition profiles described in section III-C3. ANOVAs were calculated for the two curve trials on the one hand and for the straight-line trial on the other hand.

Figure 14 shows that the average driver torque was significantly influenced by the transition profile ($F(3,48) = 73.4$, $p < 0.001$ for the curved scenario and $F(3,48) = 332.1$, $p < 0.001$ for the straight-line scenario). The effect in the straight-line scenario resides in a higher average torque for Transition 4 than for the others ($p < 0.001$ in all cases). In the curved scenario, the different profiles are more distinct. Transition 1 resulted in a lower average driver torque than for the other transitions ($p < 0.05$ compared to Transition 2; $p < 0.001$ compared to Transitions 3 and 4). On the other hand, the driver torque observed with Transition 4 was higher than for the other transitions ($p < 0.001$). Further, it can be seen in Figure 12 that the driver torque is almost identical before the obstacle for transitions 1 and 2 but is lower in the case of Transition 1 after the obstacle. This is consistent with the evolution of the sharing level: for Transition 1, the assistance continued to deliver a large part of the steering torque needed to take the turn, whereas for Transition 2 the participants had to deliver that torque and return to the initial lane after avoiding the obstacle. To see in more details how these torques evolved, we can observe the positive and negative driver workload.

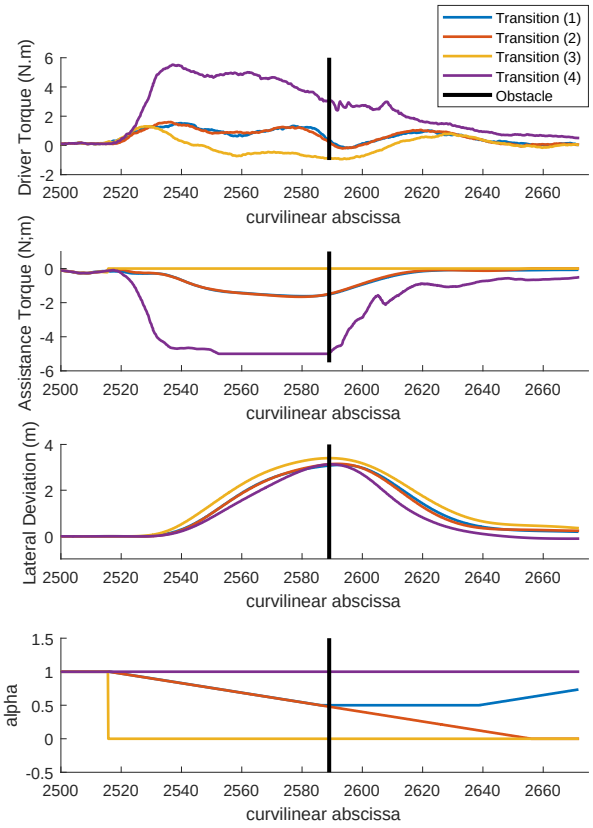


Fig. 13. Driver torque, assistance torque, and lateral deviation averaged across participants as a function of the road curvilinear abscissa in the straight-line scenaro. The sharing level is shown in the bottom graph.

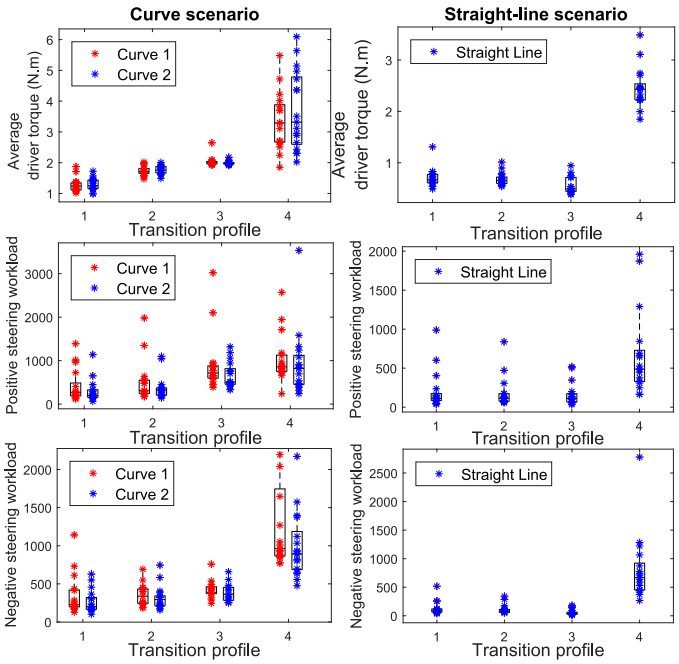


Fig. 14. Positive and negative steering workload, and average driver torque in the curve scenarios on the left and in the straight-line scenario on the right

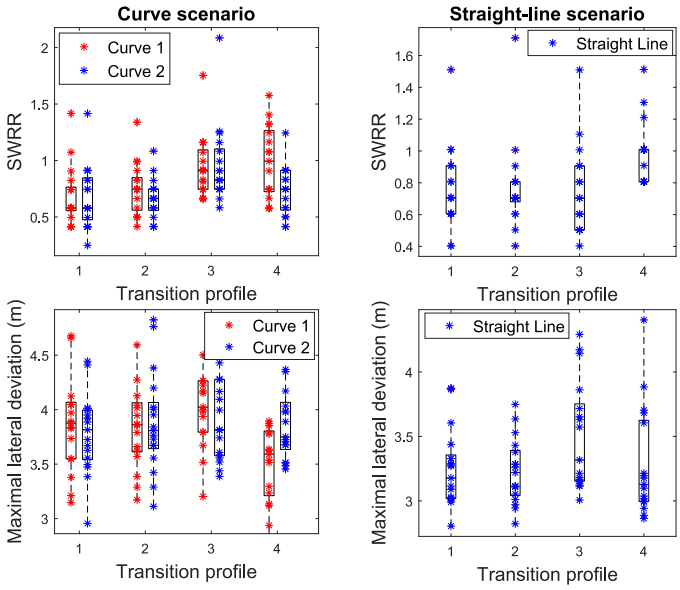


Fig. 15. SWRR and maximum lateral deviation in the curve scenarios on the left and in the straight-line scenario on the right

Figure 14 also shows that transition profiles had a significant effect on positive steering workload ($F(3,48) = 15.5$, $p < 0.001$ for the curve scenarios and $F(3,48) = 23.6$, $p < 0.001$ for the straight-line scenario) and negative steering workload ($F(3,48) = 42.0$, $p < 0.001$ for the curve scenarios and $F(3,48) = 31.9$, $p < 0.001$ for the straight-line scenario). Multiple comparison tests show that negative steering workload was larger for Transition 4 than for other transition profiles for all scenarios ($p < 0.001$), which indicates that participants resisted the assistance more during Transition 4 than in other transition profiles. For positive driver workload, there is a difference between curve and straight-line scenarios. For curve scenarios, positive driver workload is larger for Transitions 3 and 4 than for Transitions 1 and 2 ($p \leq 0.01$) whereas for the straight-line scenario, positive driver workload is only larger for Transition 4 ($p < 0.001$). These results show that in both scenarios the driver had to provide more torque for Transition 4 than for the other profiles. In the curve scenario only, the driver also had to provide more torque for Transition 3 than for Transitions 1 and 2 as there was no assistance during the curve.

The transition profile had a significant effect on the SWRR ($F(3,48) = 8.7$, $p < 0.001$ for curve scenarios and $F(3,48) = 9.3$, $p < 0.001$ for straight-line scenario; Figure 14). For the curve scenario, multiple comparison tests show that SWRR was higher for Transition 3 than for Transition 1 and 2 ($p \leq 0.001$ for Transition 3 compared with Transition 1 and 2). It was also higher for Transition 4 than for Transition 1 ($p = 0.03$). For the straight-line scenario, these tests show that SWRR was higher in the case of Transition 4 than in other transition cases ($p \leq 0.001$ when compared with other profiles).

Another significant effect of the transition profile was found on the maximum lateral deviation ($F(3,48) = 3.1$, $p = 0.036$ for the curve scenarios and $F(3,48) = 5.1$, $p = 0.004$ for the

straight-line scenario; see Figure 15). For the curve scenario, posthoc tests revealed that the maximum lateral deviation was larger in Transition 3 than in Transition 4 ($p = 0.02$). In the straight-line scenario, the maximum lateral deviation was larger in Transition 3 than in all other cases ($p < 0.05$). Thus, when no assistance torque was present, drivers made a slightly larger lateral deviation to avoid the obstacle. However, the avoidance paths remained relatively close in all conditions, especially in the straight line (Figure 13). In the bend, an initial deviation in the opposite direction due to the absence of assistance was observed for Transition 3. This is shown in Figure 12, where the average lateral deviation curve shows negative values for some time at the beginning of the manoeuvre. This is due to the sudden removal of the assistance torque after the takeover request. As participants were in a curve when it happened, the vehicle moved towards the outer-edge line of the road, and participants then had to swerve back toward the lane centre and beyond to avoid the obstacle. This explains the spike at the beginning of the driver torque curve in Figure 12.

Finally, there was no significant effect of the repetition of the curve scenario for the maximum absolute lateral deviation, and the mean absolute driver torque (we obtained $F(1,16) = 0.6$, $p = 0.47$; and $F(1,16) = 1.9$, $p = 0.18$, respectively). However, repetition had a significant effect on the positive and the negative steering workload ($F(1,16) = 24.0$, $p < 0.001$ and $F(1,16) = 13.4$, $p = 0.002$). Posthoc tests show that there is a significant reduction of the negative steering workload for Transition 4 between the first and the second curve trials, which indicates that the driver resisted the action of the system to a lesser extent. For positive steering workload, there was no significant posthoc difference. The repetition of the curve scenario also had a significant effect on the SWRR ($F(1,16) = 6.3$, $p = 0.02$). According to multiple comparison tests, SWRR was higher for the first curve trial than for the second one in the case of Transition 4 ($p = 0.009$).

### 2) Subjective indicators

Responses to the four questions posed to participants after experiencing each transition profile were analysed. Figure 16 shows that the transition profile had a significant effect on these data ($F(3.48) = 15{,}7$, $p < 0.001$ for the first question; $F(3.48) = 13{,}2$, $p < 0.001$ for the second question; $F(3.48) = 33{,}3$, $p < 0.001$ for the third question; and $F(3.48) = 7{,}3$, $p < 0.001$ for the last question). Transitions 3 and 4 were significantly different from Transitions 1 and 2 for Questions 1, 2, and 4 ($p < 0.01$ in all cases). For these three questions, Transitions 3 and 4 were not significantly different from each other, and nor were Transitions 1 and 2. This means that participants found Transitions 3 and 4 to be less smooth, less useful and less safe than Transitions 1 and 2. For Question 3, Transition 4 was significantly different from all other transitions ($p < 0.001$). Participants therefore found Transition 4 more intrusive compared to the others, which is consistent with the objective steering workload indicator in Figure 14.

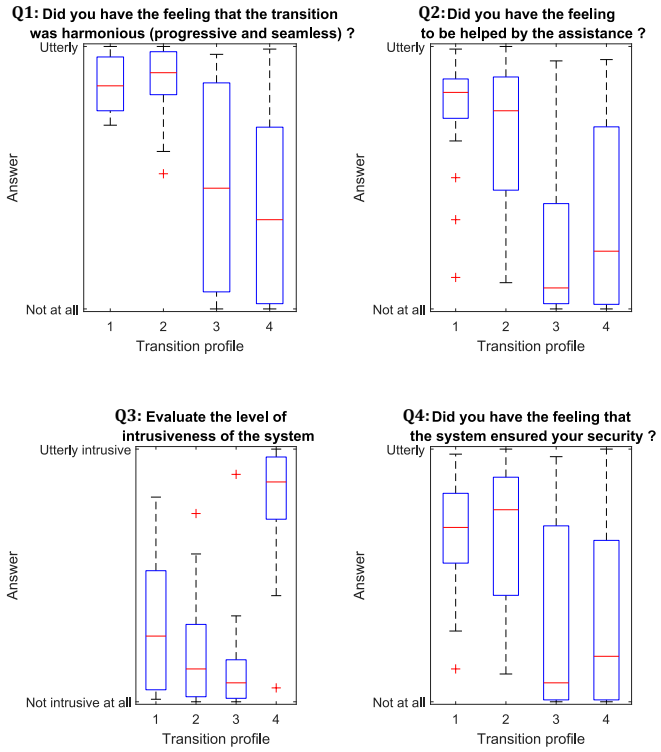


Fig. 16. Answer to questions on a Likert scale from 0 to 10

## C. Discussion

The objective of this study was to validate the relevance of the HSC strategy developed in [20] to achieve transitions between autonomous and manual control. This was done first by analysing the effective sharing of control between driver and automation during a long transition and then by comparing different transition profiles during obstacle avoidance in straight lines and curves. In the first experimental phase, we observed the ability of the system to perform transitions when the driver and the assistant had compatible reference trajectories at all times. On the other hand, in the second experimental phase, the driver deviated from the reference trajectory of the assistance and it was necessary to quickly give back the control of the steering wheel.

The first phase of the study showed that the actual level of sharing during the simulation followed the requested level of sharing. Drivers gradually gave way to the assistance system as the level of sharing increased. They also gradually increased their steering activity when they returned to manual control. The second phase confirms these results, as it has been shown that smooth transitions (Transitions 1 and 2) are more effective in terms of both steering performance and subjective feeling than a binary transition to manual control (Transition 3) or having to override the autonomous mode (Transition 4). This was particularly true when the transition occurred during a turn. These results support the idea that the HSC strategy proposed in [20] is a valid candidate to facilitate transitions between manual and autonomous modes.

In the straight-line scenario, the benefit of using a gradual transition instead of a binary transition has not been

demonstrated. Indeed, the results obtained for Transitions 1, 2, and 3 were very similar. This can be explained by the fact that the action of the autonomous mode before the transition kept the vehicle well aligned on the road axis. As a result, the driver recovered manual control under ideal conditions, without the need to be assisted in their actions. In contrast, it is important to note that the driver was not hindered by the assistance system during the gradual transition even though the system continued to tend to keep the vehicle in the lane. The advantage of using a gradual transition using HSC only becomes apparent when compared to Transition 4, for which the driver had to override the action of the autonomous system. In this case, the assistance torque was significantly higher during obstacle avoidance. Although the system torque was easily overcome, the system resistance induced a higher driver torque, which adversely affected the driver's subjective assessment of the system.

In the curve scenarios, the advantage of using gradual transitions was more obvious. First of all, at the beginning of the transition, Transitions 1 and 2 provided an assisting torque that helped the driver stay on the right trajectory to follow the road while allowing the driver the freedom to deviate from it. On the contrary, in the case of a binary transition, the vehicle's trajectory was no longer supported and the driver had to correct the induced deviation. In addition, Transition 1 allows the driver's torque to be further reduced by helping the driver to return to the lane centre after obstacle avoidance. For Transition 4, the driver received lane-tracking assistance throughout the entire manoeuvre, but the torque required to override the assistance and avoid the obstacle was too high to make this system acceptable to drivers.

## V. Conclusion

This paper described a strategy to achieve transitions between manual and autonomous driving modes. This strategy is based on an HSC system that was adapted to be able to gradually modify the sharing level during the transition phase. This was then tested with real drivers on a driving simulator. The results demonstrated first that the transition strategy gives the expected results as the driver's torque corresponded to the sharing level. Second, when different transition profiles were compared, gradual transitions produced the best steering performance and the most favourable subjective evaluation.

To confirm these results, this transition strategy needs to be tested under a wider range of conditions and in a real vehicle. For example, consideration can be given to road conditions. Indeed, on icy or wet roads, some drivers will want to have full control of the car, while others will not have confidence in their own abilities and will rely much more on the system. The question of the temporality of transitions is also a central issue to be addressed, as it may depend on the use case considered and the preferences of the driver. Finally, it would be wise to compare the performance of this HSC strategy with others proposed in the literature.

## Acknowledgment

This work was supported by AutoConduct research program funded by the French ANR "Agence Nationale de la Recherche" (grant ANR-16-CE22-0007-05).

## References

[1] S. G. Klauer, T. A. Dingus, V. L. Neale, J. Sudweeks, and D. J. Ramsey, "The Impact of Driver Inattention on Near-Crash/Crash Risk: An Analysis Using the 100-Car Naturalistic Driving Study Data," *National Highway Traffic Safety Administration*, Apr. 2006.

[2] N. Kalra and S. M. Paddock, "Driving to safety: How many miles of driving would it take to demonstrate autonomous vehicle reliability?" *Transportation Research Part A: Policy and Practice*, vol. 94, pp. 182–193, Dec. 2016.

[3] J. C. F. de Winter, R. Happee, M. H. Martens, and N. A. Stanton, "Effects of adaptive cruise control and highly automated driving on workload and situation awareness: A review of the empirical evidence," *Transportation Research Part F: Traffic Psychology and Behaviour*, vol. 27, pp. 196–217, Nov. 2014.

[4] M. Young and N. Stanton, "Malleable Attentional Resources Theory: A New Explanation for the Effects of Mental Underload on Performance," *Human factors*, vol. 44, pp. 365–75, Feb. 2002.

[5] O. Carsten, F. Lai, Y. Barnard, A. Jamson, and N. Merat, "Control Task Substitution in Semiautomated Driving: Does It Matter What Aspects Are Automated?" *Human factors*, vol. 54, pp. 747–61, Oct. 2012.

[6] S. Casner, E. Hutchins, and D. Norman, "The Challenges of Partially Automated Driving," *Communications of the ACM*, vol. 59, p. 70, May 2016.

[7] N. Merat, A. H. Jamson, F. C. H. Lai, and O. Carsten, "Highly Automated Driving, Secondary Task Performance, and Driver State," *Human Factors: The Journal of the Human Factors and Ergonomics Society*, vol. 54, no. 5, pp. 762–771, Oct. 2012.

[8] C. M. Rudin-Brown and H. A. Parker, "Behavioural adaptation to adaptive cruise control (ACC): implications for preventive strategies," *Transportation Research Part F: Traffic Psychology and Behaviour*, vol. 7, no. 2, pp. 59–76, Mar. 2004.

[9] B. Seppelt and T. Victor, "Potential Solutions to Human Factors Challenges in Road Vehicle Automation," in *Road Vehicle Automation 3*, Jul. 2016, pp. 131–148.

[10] C. Mole, O. Lappi, O. Giles, G. Markkula, F. Mars, and R. Wilkie, "Getting Back Into the Loop: The Perceptual-Motor Determinants of Successful Transitions out of Automated Driving," *Human Factors The Journal of the Human Factors and Ergonomics Society*, vol. 61, Jan. 2019.

[11] N. Merat, A. H. Jamson, F. C. H. Lai, M. Daly, and O. M. J. Carsten, "Transition to manual: Driver behaviour when resuming control from a highly automated vehicle," *Transportation Research Part F: Traffic Psychology and Behaviour*, vol. 27, no. Part B, pp. 274–282, Nov. 2014.

[12] B. K. J. Mok, M. Johns, K. J. Lee, H. P. Ive, D. Miller, and W. Ju, "Timing of unstructured transitions of control in automated driving," in *2015 IEEE Intelligent Vehicles Symposium (IV)*, Jun. 2015, pp. 1167–1172.

[13] T. Vogelpohl, M. Kühn, T. Hummel, T. Gehlert, and M. Vollrath, "Transitioning to manual driving requires additional time after automation deactivation," *Transportation Research Part F: Traffic Psychology and Behaviour*, vol. 55, pp. 464–482, May 2018.

[14] M. Mulder, D. A. Abbink, M. M. v. Paassen, and M. Mulder, "Design of a Haptic Gas Pedal for Active Car-Following Support," *IEEE Transactions on Intelligent Transportation Systems*, vol. 12, no. 1, pp. 268–279, Mar. 2011.

[15] M. Mulder, D. A. Abbink, and E. R. Boer, "Sharing Control With Haptics: Seamless Driver Support From Manual to Automatic Control," *Human Factors*, vol. 54, no. 5, pp. 786–798, Oct. 2012.

[16] K. Okada, K. Sonoda, and T. Wada, "Control Transfer Method from Automated Driving to Manual Driving During Curve Travel," in *2019 IEEE International Conference on Systems, Man and Cybernetics (SMC)*, Oct. 2019, pp. 3130–3135, iSSN: 1062-922X.

[17] T. Wada, K. Sonoda, T. Okasaka, and T. Saito, "Authority transfer method from automated to manual driving via haptic shared control," in *2016 IEEE International Conference on Systems, Man, and Cybernetics (SMC)*, Oct. 2016, pp. 002 659–002 664.

[18] T. Saito, T. Wada, and K. Sonoda, "Control Authority Transfer Method for Automated-to-Manual Driving via Shared Authority Mode," *IEEE Transactions on Intelligent Vehicles*, vol. PP, no. 99, pp. 1–1, 2018.

[19] J. Ludwig, A. Haas, M. Flad, and S. Hohmann, "A Comparison of Concepts for Control Transitions from Automation to Human," in *2018 IEEE International Conference on Systems, Man, and Cybernetics (SMC)*, Oct. 2018, pp. 3201–3206.

[20] B. Pano, P. Chevrel, and F. Claveau, "Anticipatory and Compensatory e-Assistance for Haptic Shared Control of the Steering Wheel," in *2019 18th European Control Conference (ECC)*, Jun. 2019, pp. 724–731.

[21] L. Saleh, P. Chevrel, F. Claveau, J. Lafay, and F. Mars, "Shared Steering Control Between a Driver and an Automation: Stability in the Presence of Driver Behavior Uncertainty," *IEEE Transactions on Intelligent Transportation Systems*, vol. 14, no. 2, pp. 974–983, Jun. 2013.

[22] D. A. Abbink, M. Mulder, and E. R. Boer, "Haptic shared control: smoothly shifting control authority?" *Cognition, Technology & Work*, vol. 14, no. 1, pp. 19–28, Mar. 2012.

[23] F. Mars and P. Chevrel, "Modelling human control of steering for the design of advanced driver assistance systems," *Annual Reviews in Control*, vol. 44, pp. 292–302, Jan. 2017.

[24] D. Salvucci and R. Gray, "A two-point visual control model of steering," *Perception*, vol. 33, pp. 1233–48, Feb. 2004.

[25] L. Saleh, "Contrôle Latéral Partagé d'un Véhicule Automobile," phdthesis, Ecole Centrale de Nantes (ECN), Apr. 2012.

[26] L. Saleh, P. Chevrel, F. Mars, J.-F. Lafay, and F. Claveau, "Human-like cybernetic driver model for lane keeping," *IFAC Proceedings Volumes*, vol. 44, no. 1, pp. 4368–4373, Jan. 2011.

[27] L. Saleh, P. Chevrel, and J.-F. Lafay, "Generalized H2-Preview Control and its Application to Car Lateral Steering," *IFAC Proceedings Volumes*, vol. 43, no. 2, pp. 132–137, Jan. 2010.

[28] N. Nagai, Y. Takeuchi, and K. Teranishi, "Handling and stability evaluation of four-wheel-steered vehicles considering steering torque - angle relation," *JSAE Review*, vol. 13, no. 3, Jul. 1992.

[29] L. Liu, M. Nagai, and P. Raksincharoensak, "On Torque Control of Vehicle Handling and Steering Feel for Avoidance Maneuver with Electric Power Steering," *IFAC Proceedings Volumes*, vol. 41, no. 2, pp. 12 073–12 078, Jan. 2008.

[30] A. Kirli and M. S. Arslan, "Online optimized hysteresis-based steering feel model for steer-by-wire systems," *Advances in Mechanical Engineering*, vol. 8, no. 7, Jul. 2016.

[31] C. Sentouh, A. T. Nguyen, M. A. Benloucif, and J. C. Popieul, "Driver-Automation Cooperation Oriented Approach for Shared Control of Lane Keeping Assist Systems," *IEEE Transactions on Control Systems Technology*, pp. 1–17, 2018.